

# EXPLORING THE SPECTRAL PROPERTIES OF HIGHLY ACCRETING QUASARS AT HIGH REDSHIFT

Mary Loli Martínez-Aldama<sup>1</sup> · Alenka C. Negrete<sup>2</sup> · Ascensión del Olmo<sup>1</sup> · Paola Marziani<sup>3</sup> · Jack Sulentic<sup>1</sup> ·  
Deborah Dultzin<sup>2</sup>

<sup>1</sup>Instituto de Astrofísica de Andalucía–CSIC, Spain

<sup>2</sup>Instituto de Astronomía–UNAM, Mexico

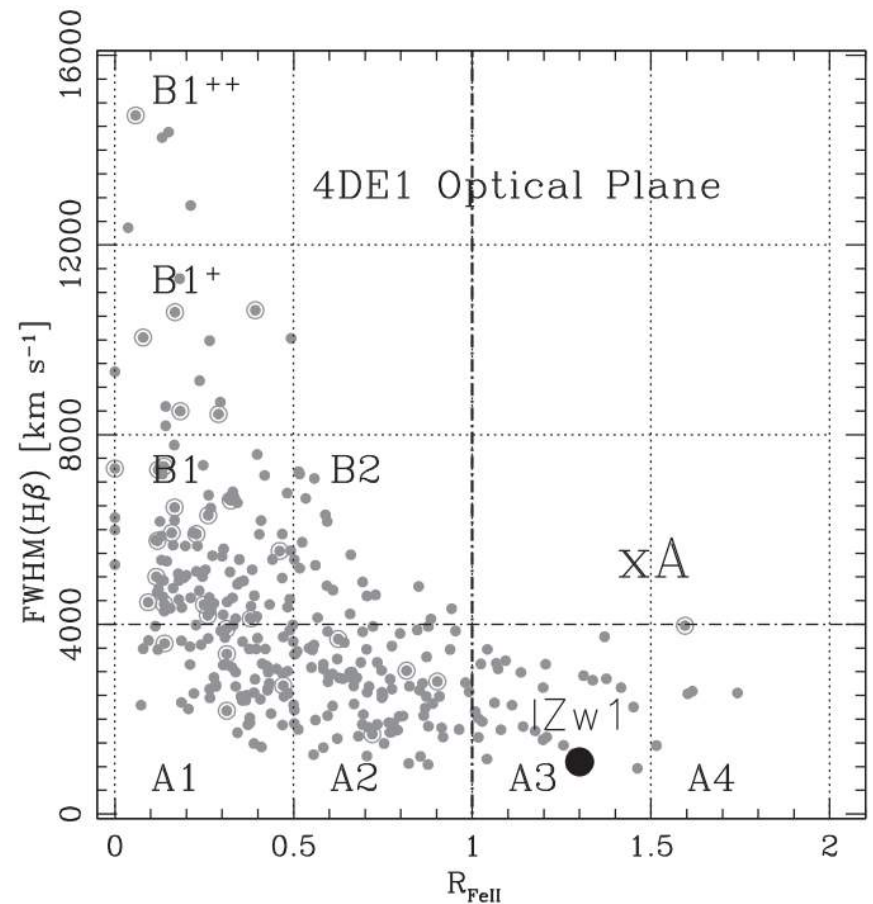
<sup>3</sup>Osservatorio Astronomico di Padova–INAF, Italy



# 4D Eigenvector 1: an evolution diagram for type 1 AGN

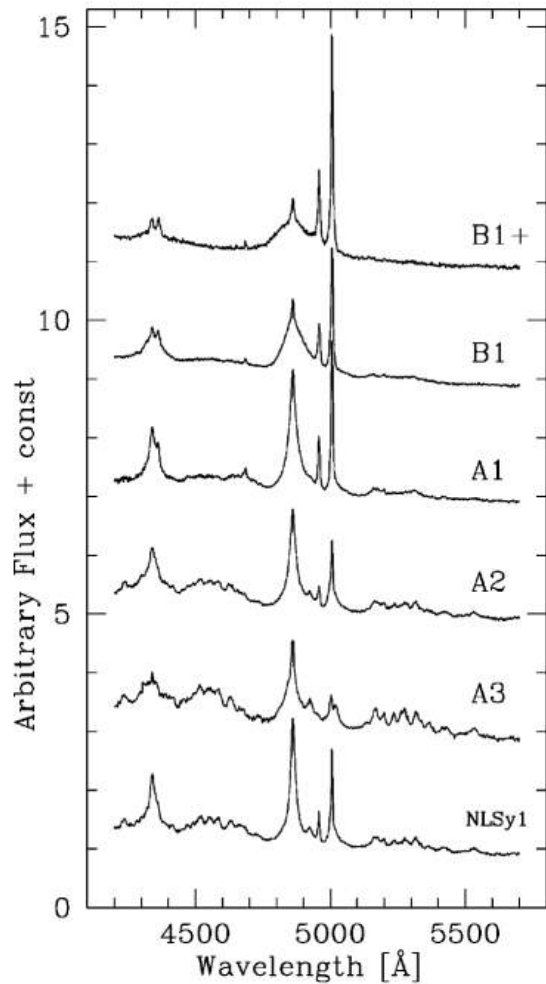
The **4D Eigenvector 1 (4DE1)** (Boroson & Green 1992; Sulentic+ 2000; Marziani+ 2001, 2003; Sulentic+ 2007, 2010, 2014) is a spectroscopic unifier/discriminator of the emission lines properties for type 1 AGN. It is based on four parameters:

- 1)  $\text{FWHM}(\text{H}\beta_{\text{BC}})$ : prototype of LILs
- 2)  $R_{\text{Fe II}} = W(\text{Fe II } \lambda 4570) / W(\text{H}\beta_{\text{BC}})$
- 3)  $\Gamma_{\text{soft}}$ : spectral index of soft X-ray
- 4) CIV  $\lambda 1549$  blueshift: prototype of HILs

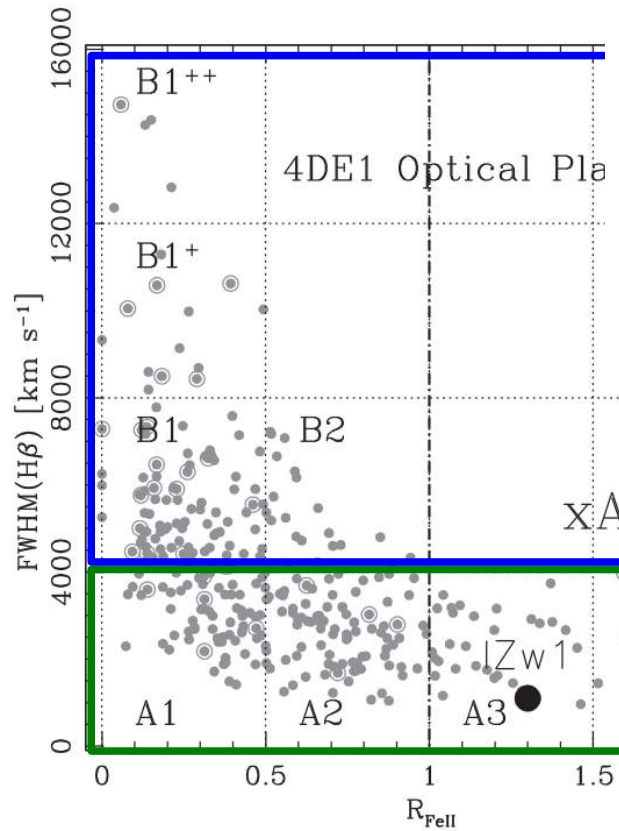


# 4D Eigenvector 1: an evolution diagram for type 1 AGN

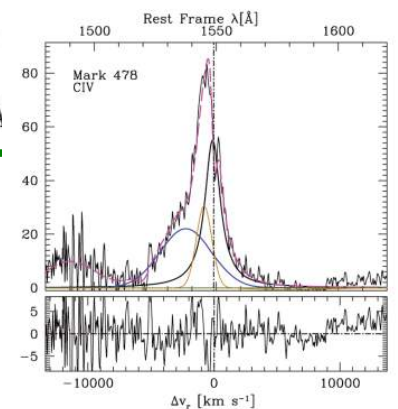
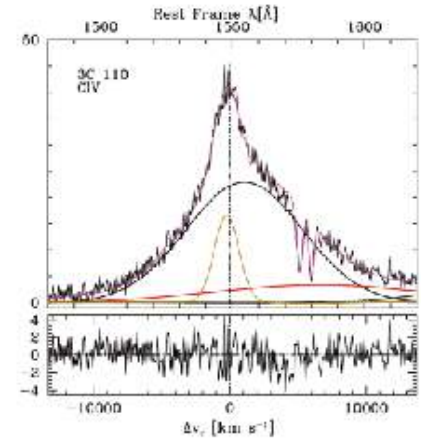
Along the 4DE1, we can find a change in the spectral properties of the AGN, suggesting the existence of two kind of populations: **A** and **B**



Sulentic+ (2002)



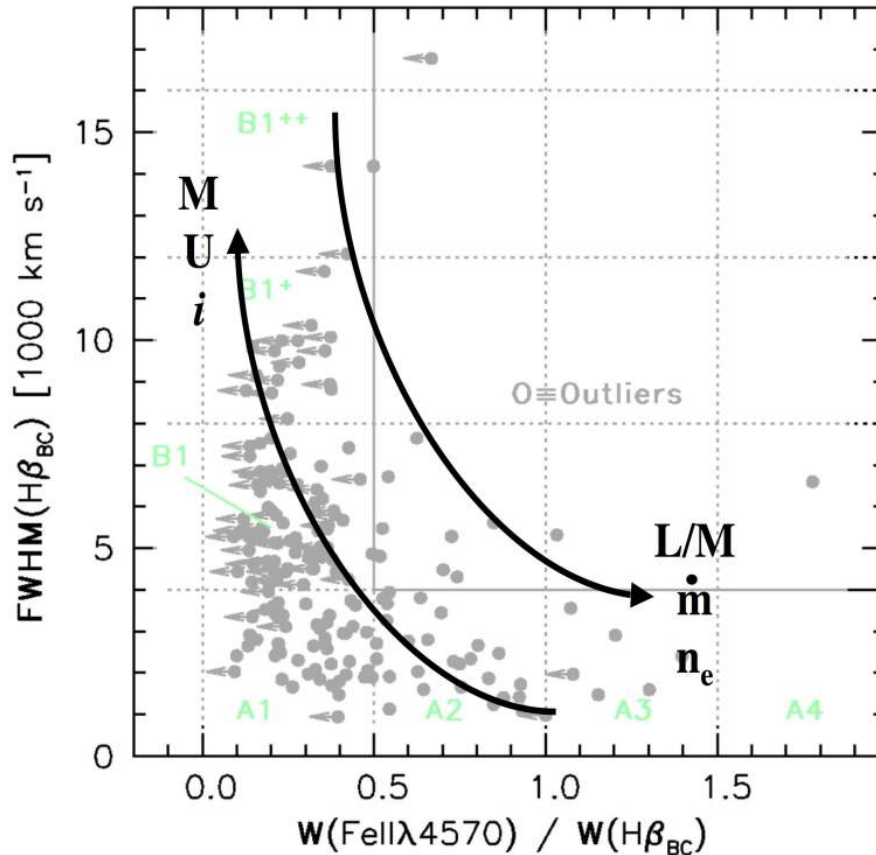
Marziani & Sulentic (2014)



4,000 km s<sup>-1</sup>

## 4D Eigenvector 1: an evolution diagram for type 1 AGN

Furthermore, the 4DE1 sequence we can find a variation of the physical parameters and in the orientation. Then, the 4D Eigenvector 1 could be considered as a “**HR diagram**” for type 1 quasars (Sulentic, Marziani & Dultzin 2000, Zamfir+ 2010).



Zamfir+ (2010)

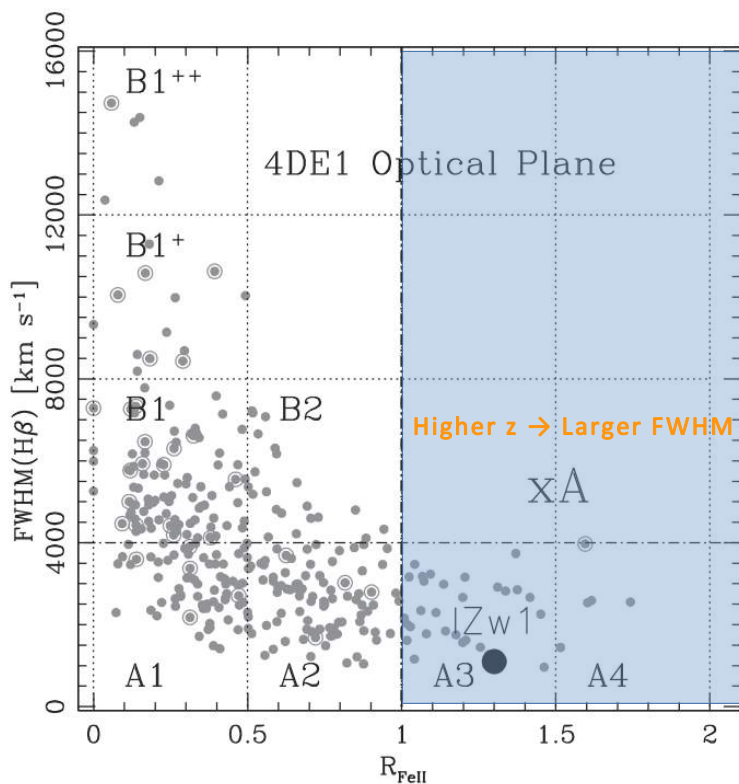
These results were confirmed by Shen & Ho (2013) using the SDSS data.

# Highly accretors AGNs along the 4DE1

Considering several UV and optical samples (Bachev+ 2004; Marziani+ 2003, 2009; Negrete+ 2012, 2013; Sulentic+ 2004, 2007, 2014), we have identified the properties for the highly accretors AGNs. They are located in the **extreme population A region**.

Optical criterion

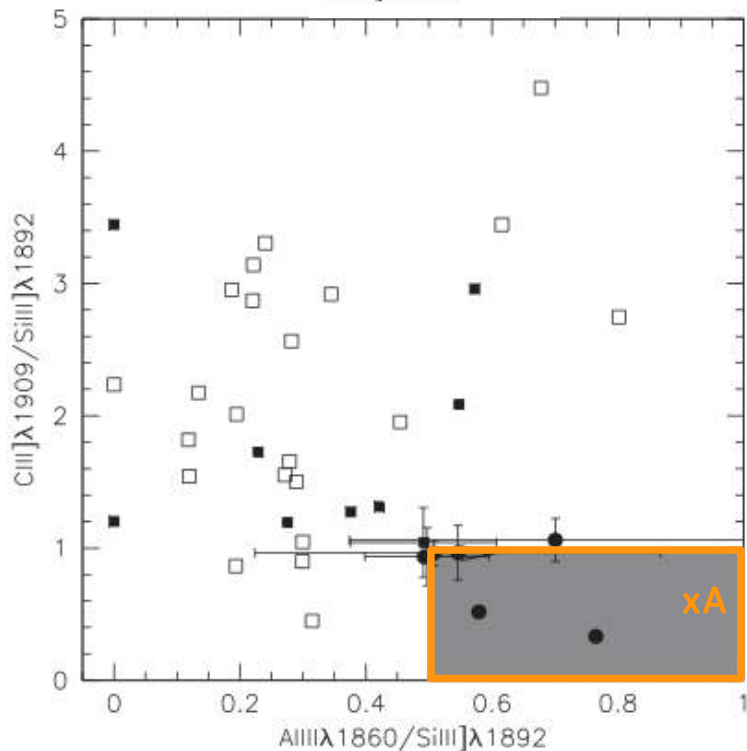
$$R_{\text{FeII}} \geq 1.0 \rightarrow \{A3, A4, \text{xA}\}$$



UV criteria

$$\frac{\text{Al III } \lambda 1860}{\text{Si III } \lambda 1892} \geq 0.5$$

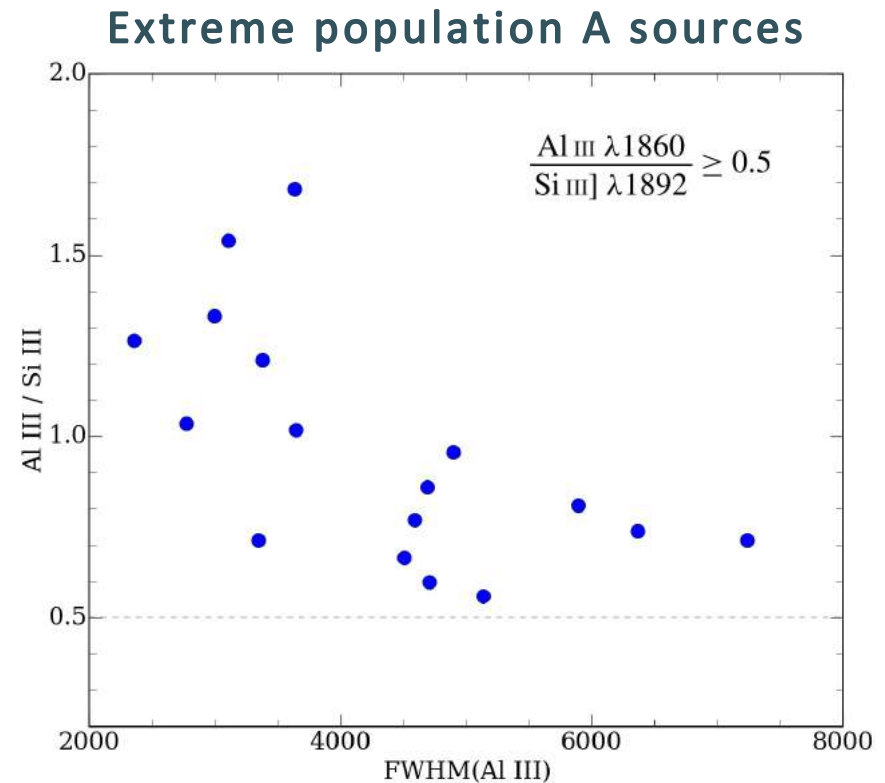
$$\frac{\text{Si III } \lambda 1892}{\text{C III } \lambda 1909} \geq 1.0$$



# GTC highly accretors sample

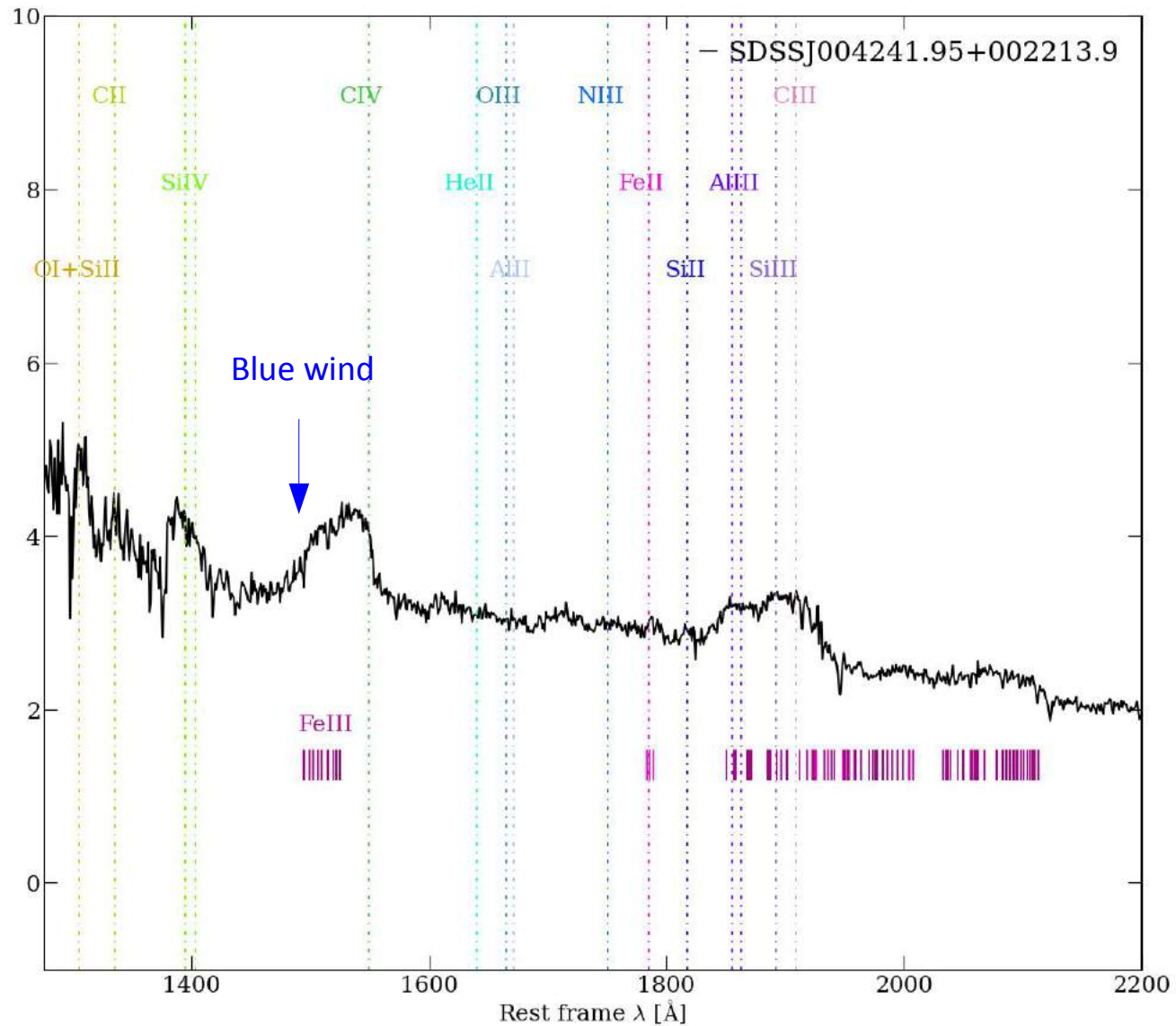
Using the **OSIRIS** spectrograph mounted in the **Gran Telescopio Canarias (GTC)**, we observed a sample of highly accretor quasars (~50 sources), which were selected with the **UV** criteria proposed by 4DE1.

<u>QSO</u>	<u>z</u>	<u>Lines used</u>
SDSSJ021606.41+011509.5	2.223585	<u>OI+SII, CII</u>
SDSSJ222753.07-092951.7	2.163938	<u>CII, Ly<math>\alpha</math></u>
SDSSJ000807.27-103942.7	2.466034	<u>OI+SII, CII, Ly<math>\alpha</math></u>
SDSSJ143525.31+400112.2	2.261532	<u>OI+SII, CII</u>
SDSSJ110022.53+484012.6	2.079899	<u>Si II 1264, OI+SII</u>
SDSSJ024154.42-004757.5	2.391897	<u>Si II 1264, OI+SII, CII</u>
SDSSJ101822.96+203558.6	2.250155	<u>Si II 1264, OI+SII</u>
SDSSJ151258.36+352533.2	2.238270	<u>OI+SII, CII</u>
SDSSJ214009.01-064403.9	2.080758	<u>Si II 1264, OI+SII, CII</u>
SDSSJ125659.79-033813.8	2.980083	<u>OI+SII</u>
SDSSJ105806.16+600826.9	2.940572	<u>OI+SII, CII</u>
SDSSJ103527.40+445435.6	2.263917	<u>OI+SII</u>
SDSSJ084036.16+235524.7	2.184233	<u>OI+SII, CII</u>
SDSSJ004241.95+002213.9	2.056166	<u>OI+SII, CII</u>
SDSSJ131132.92+052751.2	2.123420	<u>OI+SII, CII</u>
SDSSJ144412.37+582636.9	2.345544	<u>Si II 1264, OI+SII</u>
SDSSJ234657.25+145736.0	2.170262	<u>Si II 1264, CII</u>
SDSSJ220119.62-083911.6	2.183952	<u>Al III, CII, Si II</u>
SDSSJ233132.83+010620.9	2.627299	<u>Al III, CII, Si II</u>

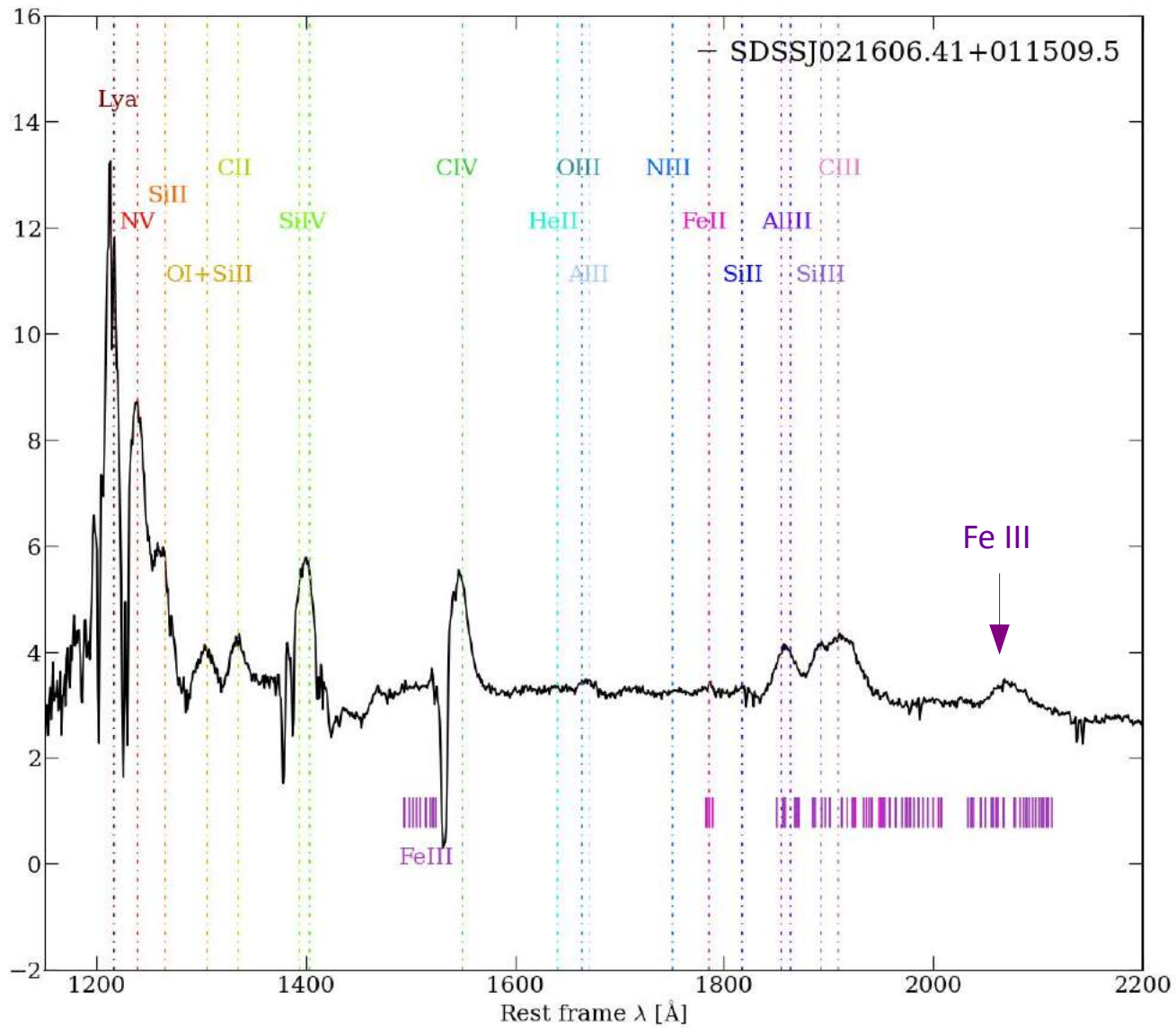




# Some examples: strong blueshifted CIV component



# Some examples: Broad Absorption Line QSO

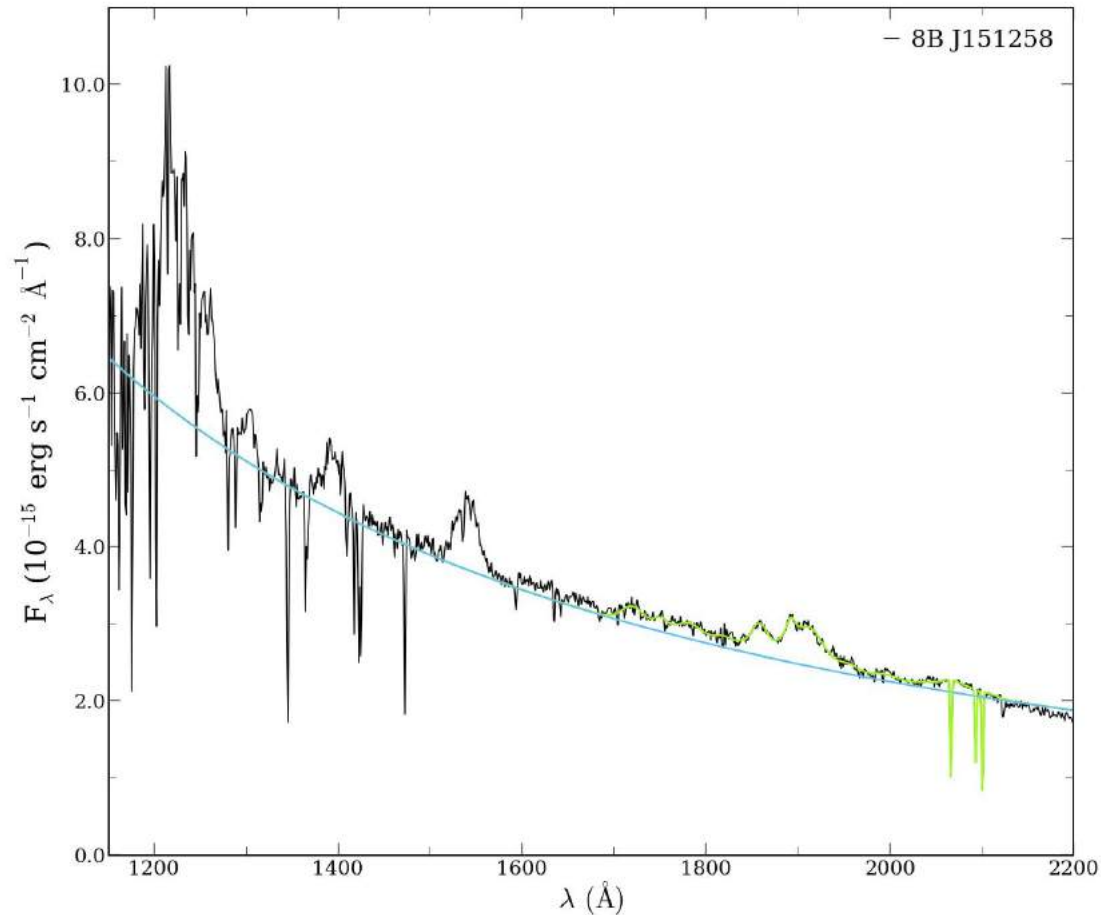




# Multicomponents fits

Following the 4DE1 context we performed multicomponents fit to separate the different contributions.

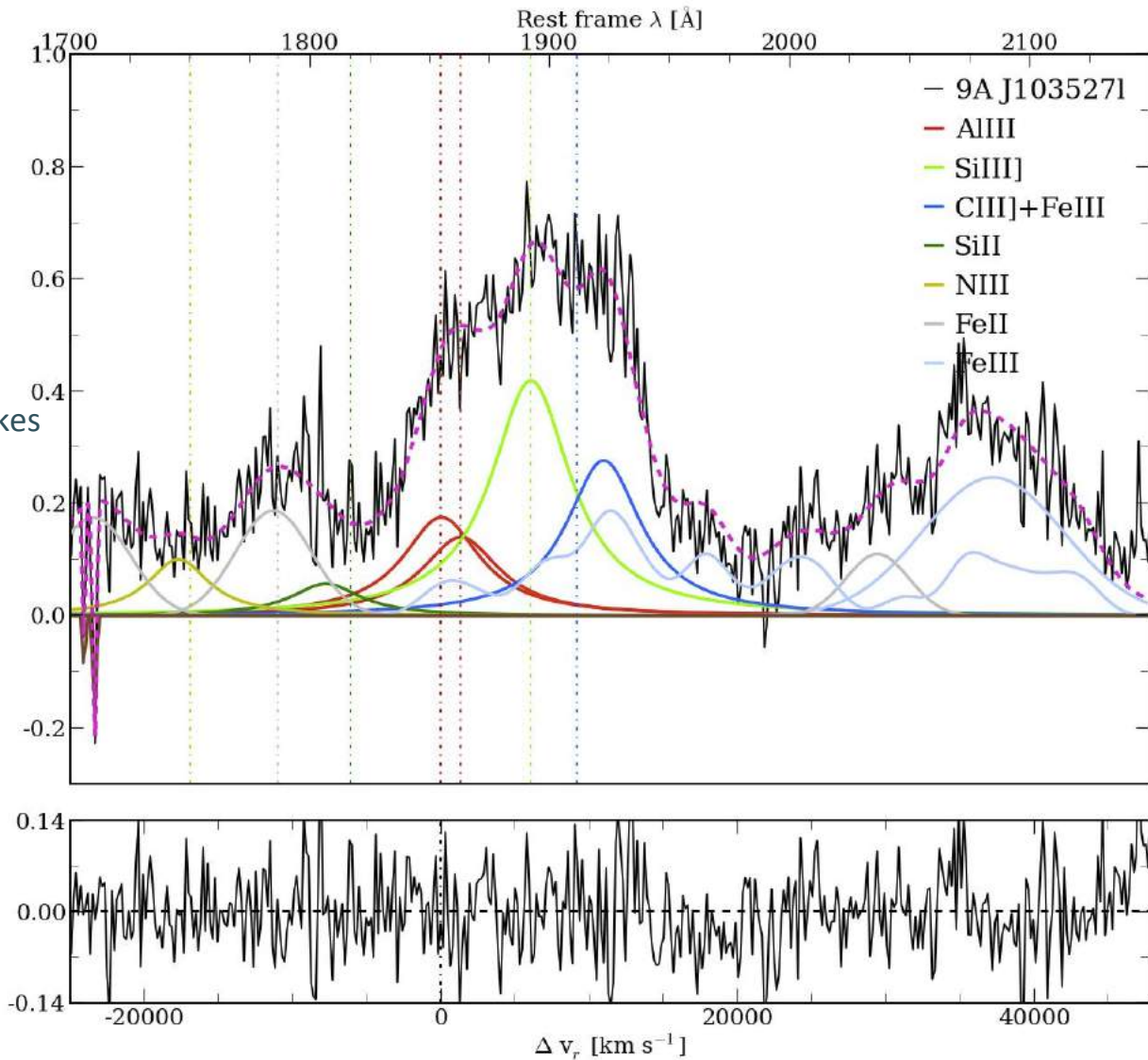
- Fitting criteria
- Continuum: local or global
  - Pop. A: lorentzian profiles
  - Low Ionization Lines: BC
  - High Ionization Lines: BC+Blueshift



# Multicomponents fits: Blend 1900 Å

## Blend 1900: 1700-2150 Å

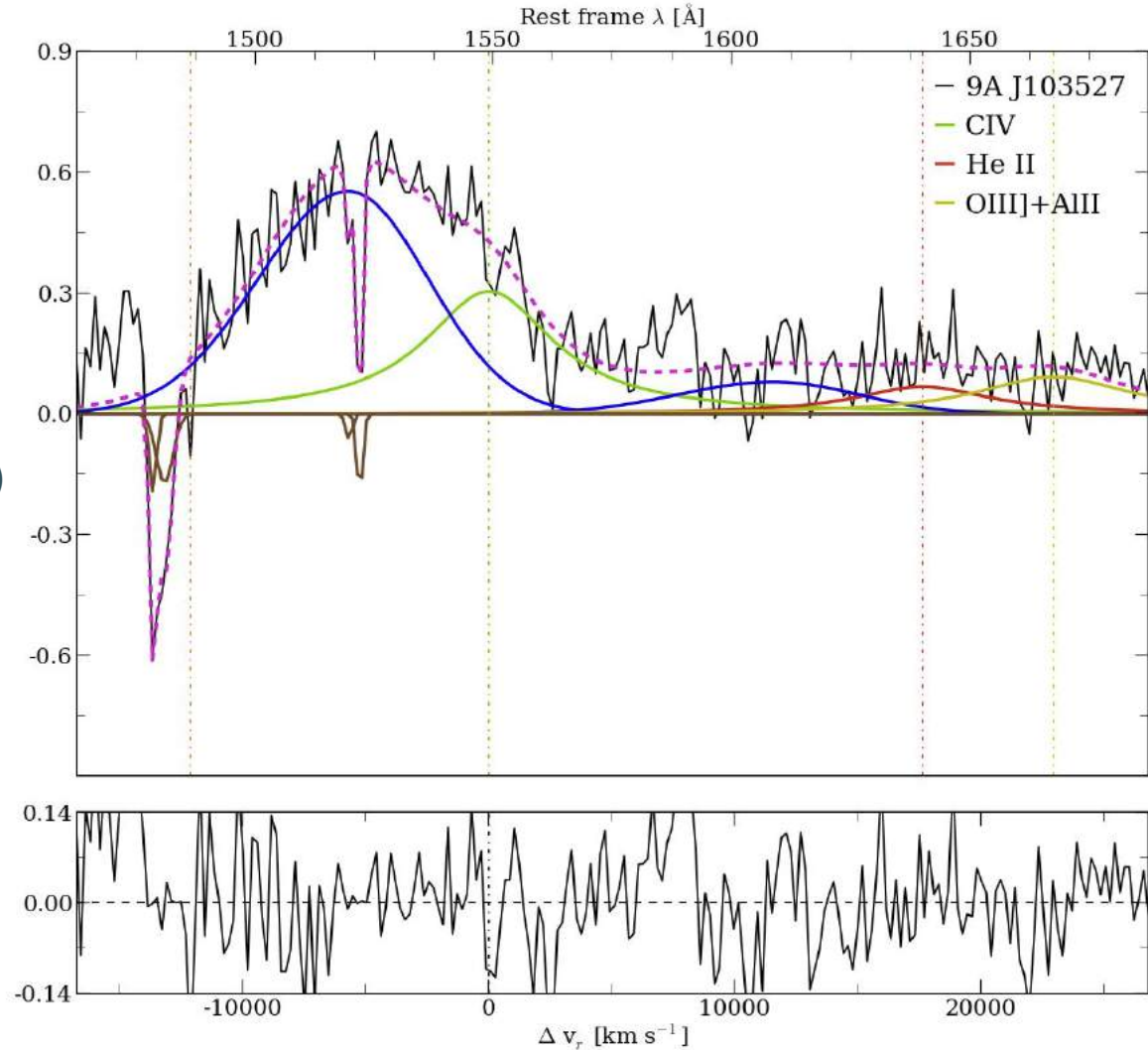
- Al III]  $\lambda$ 1860
- Si III]  $\lambda$ 1892
- C III]  $\lambda$ 9009
- Si II  $\lambda$ 1816
- N III  $\lambda$ 1750
- Fe II: isolated gaussians  
at 1715, 1785,  
2020 Å
- Fe III: Vestergaard & Wilkes  
(2001) + 2080 Å



# Multicomponents fits: CIV $\lambda 1549$

## CIV region: 1500-1700 Å

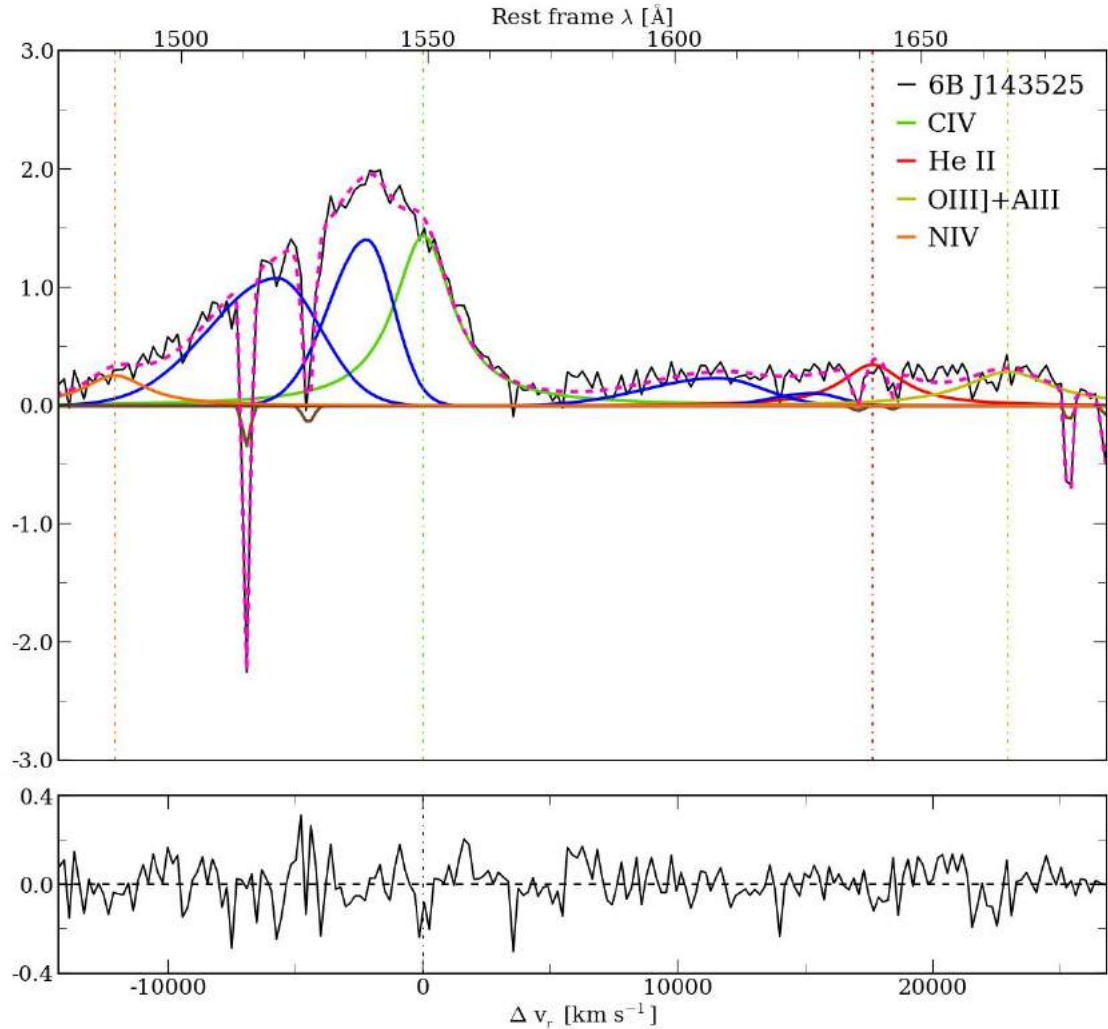
- C IV  $\lambda 1549$ : BC+Blueshift (2)
- He II  $\lambda 1640$ : BC+Blueshift (2)
- OIII]  $\lambda 1664$  + Al II  $\lambda 1670$
- N IV  $\lambda 1486$



# Multicomponents fits: CIV $\lambda 1549$

## CIV region: 1500-1700 Å

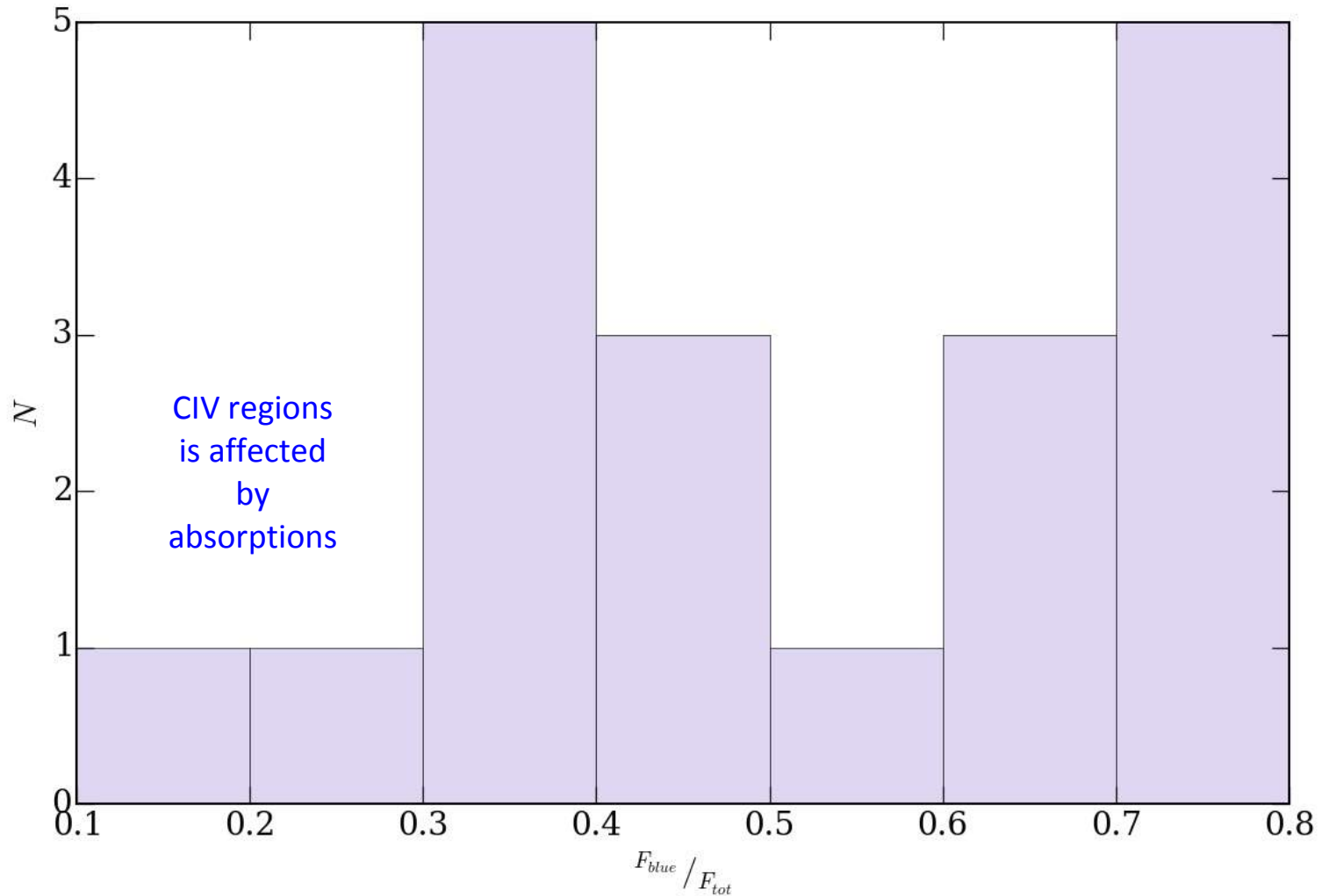
- C IV  $\lambda 1549$ : BC+Blueshift (2)
- He II  $\lambda 1640$ : BC+Blueshift (2)
- OIII]  $\lambda 1664$  + Al II  $\lambda 1670$
- N IV  $\lambda 1486$



# CIV $\lambda 1549$ outflows



If we compare the contribution of the CIV  $\lambda 1549$  blue component respect to the total contribution, we find a contribution of more than 40% for the 65% of the sources.



# Photoionization method

Considering the flux ratios of the UV lines, we can determine  $U$  and  $n_H$  using a photoionization model. And then, getting the size of the Broad Line Region,  $r_{BLR}$  (Negrete+ 12,13,14).

Ionization parameter

$$U = \frac{\int_{\nu_0}^{+\infty} \frac{L_\nu}{h\nu} d\nu}{4\pi n_H c r^2}$$

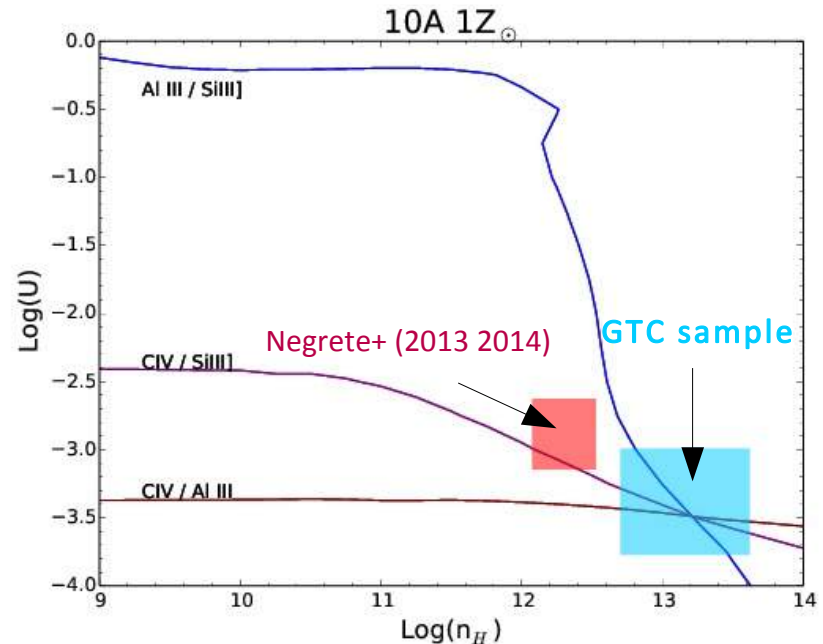
Broad Line Region size

$$r_{BLR} = \left[ \frac{\int_{\nu_0}^{+\infty} \frac{L_\nu}{h\nu} d\nu}{4\pi U n_H c} \right]^{1/2}$$

CLOUDY (Ferland+ 2013) input conditions:

- Mathews & Ferland continuum (1987)
- $N_c = 10^{23-25} \text{ cm}^{-2}$
- $1Z_\odot, 5Z_\odot$
- $4 \leq \log(U) \leq 0$
- $9 \leq \log(n_H) \leq 14$

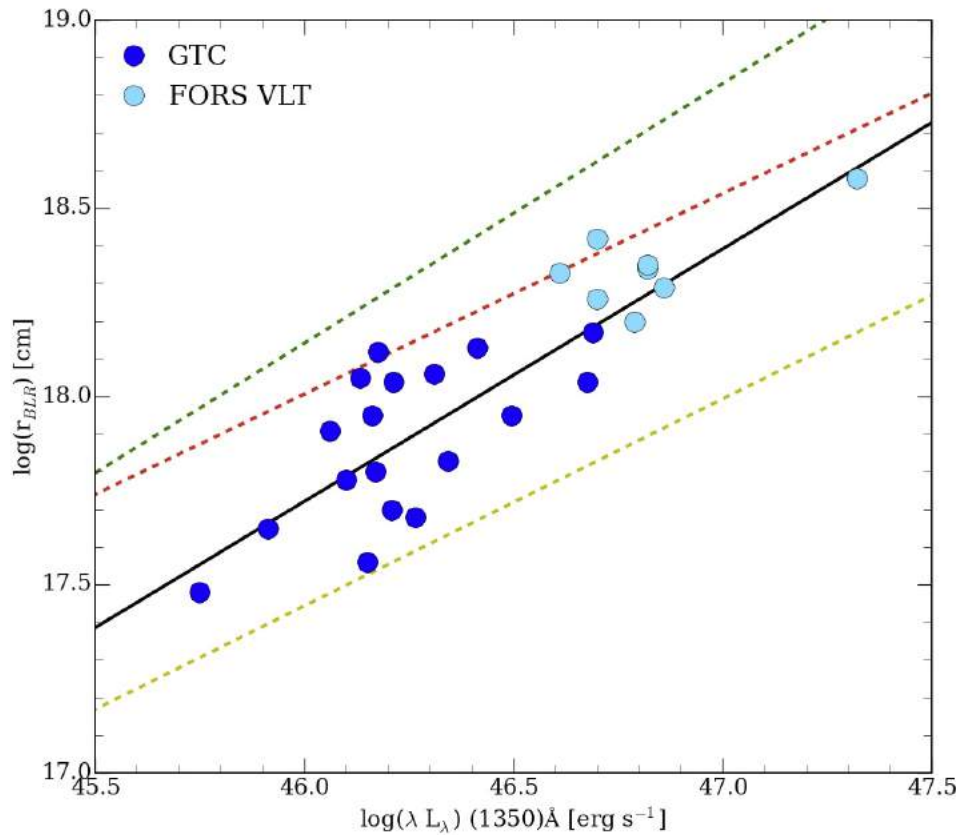
SDSSJ084036.16+235524.7,  $1Z_\odot$





# Broad Line Region size

Considering a small high-z sample but not highly accretor (Negrete+ 2012, 2013), we find that the tendency previously found for the  $r_{BLR}$  size is in agreement with our results and the BLR radii is smaller than the computing with the RM methods.



Photionization model

- Negrete+ (2012)

$$r_{BLR} = \frac{1}{h^{(1/2)}c} (UN_e)^{(1/2)} \left( \int_0^{\lambda_{Ly}} f_{\lambda} \lambda d\lambda \right)^{(1/2)} d_p$$
  

Reverberation mapping

$5100 \cdot L_{5100}$

- Vestergaard+ (2005): H $\beta$

$$\frac{R_{BLR}}{10 \text{ lt-days}} = (2.23 \pm 0.21) \left[ \frac{\lambda L_{\lambda}(5100 \text{ \AA})}{10^{44} \text{ ergs s}^{-1}} \right]^{0.69 \pm 0.05}$$

- Kaspi+ (2007): CIV  $\lambda 1549$

$$\log(R_{BLR}/1 \text{ lt-day}) = 1.527^{+0.031}_{-0.031} + 0.533^{+0.035}_{-0.033} \log(\lambda L_{\lambda}/10^{44} L_{\odot})$$

- Bentz+ (2013): H $\beta$

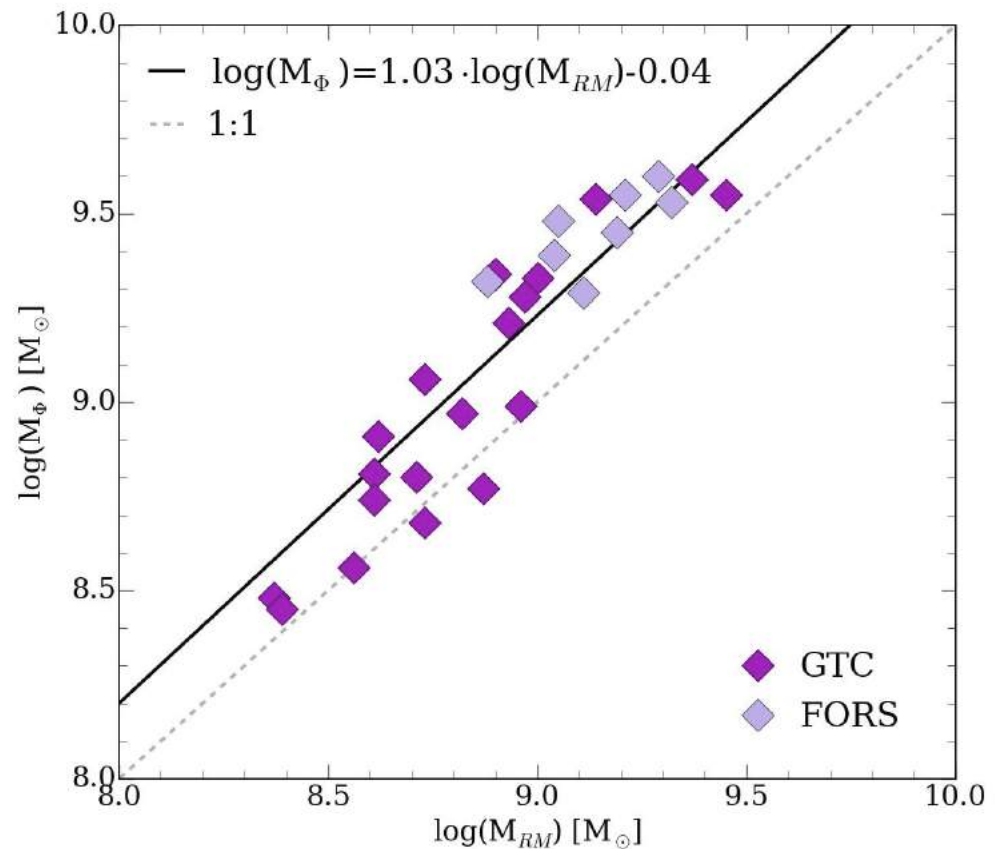
$$\frac{R_{BLR}}{10 \text{ lt-days}} = (0.24 \pm 0.06) \left[ \frac{\lambda L_{\lambda}(1350 \text{ \AA})}{10^{43} \text{ ergs s}^{-1}} \right]^{0.55 \pm 0.04}$$

# Black hole mass determination

Computing the black hole mass using  $r_{BLR}$  the found, we get that the mass obtained from the photoionization models (GTC+FORs) is slightly higher than the obtained from reverberation mapping.

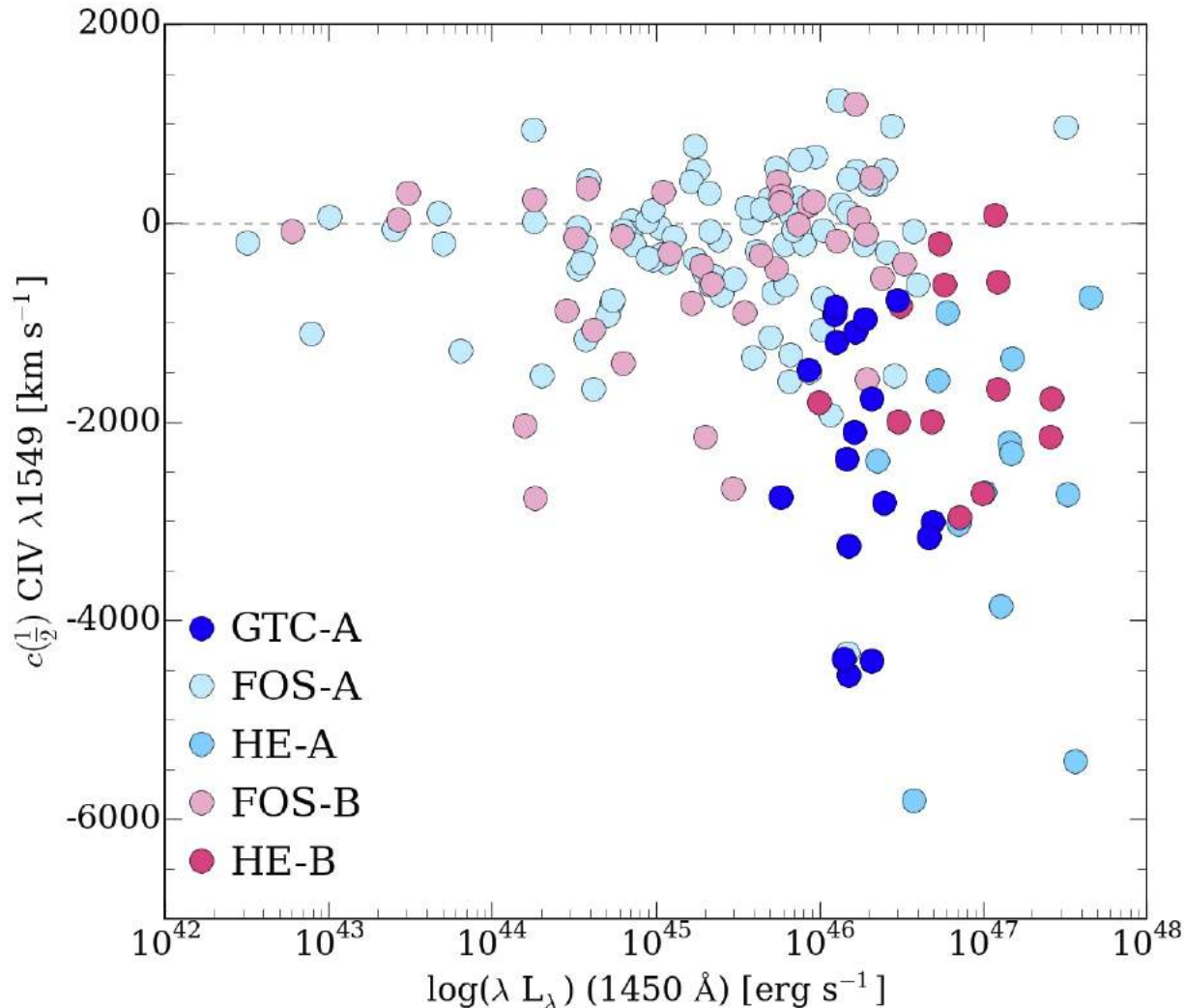
$$M_{BH,\Phi} \left\{ \begin{array}{l} \text{Negrete (2012)} \\ M = \frac{3}{4G} f_{0.75} r_{BLR} (FWHM)^2 \end{array} \right.$$
  

$$M_{BH,RM} \left\{ \begin{array}{l} \text{Vestergaard \& Peterson (2006)} \\ \log M_{BH}(C\ IV) = \log \left\{ \left[ \frac{FWHM(C\ IV)}{1000\ km\ s^{-1}} \right]^2 \left[ \frac{\lambda L_{\lambda}(1350\ \text{\AA})}{10^{44}\ \text{ergs}\ s^{-1}} \right] \right. \\ \left. + (6.66 \pm 0.01) \right. \end{array} \right.$$



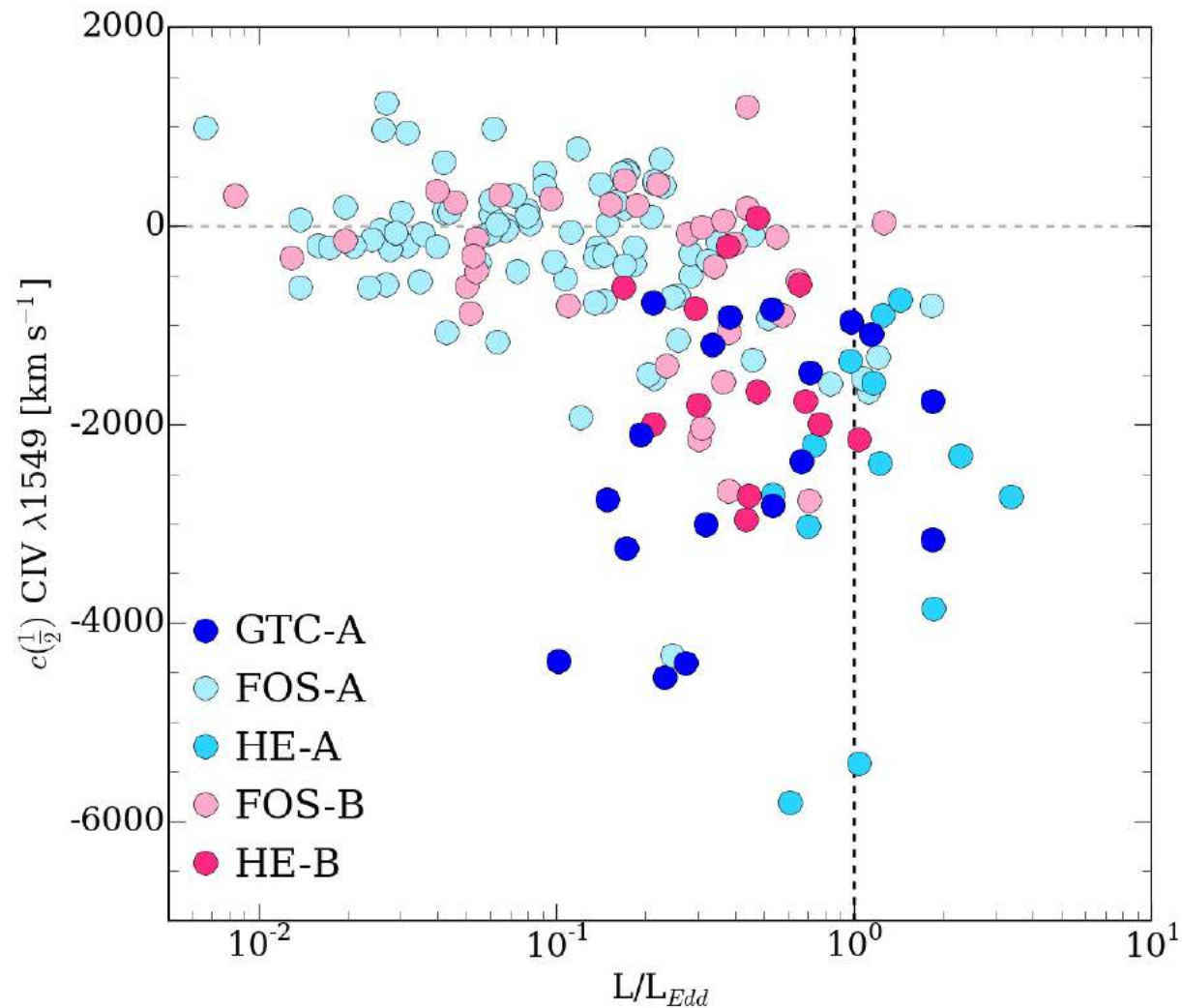
# CIV $\lambda 1549$ outflows and the Eddington ratios

Considering two samples (FORS VLT+HE) with **Pop. A** and **B sources** (Marziani & Sulentic 2014; Sulentic+ 2004, 2006, 2007; Marziani+ 2009), we find a strong tendency to the Pop. A sources to show CIV outflows, specially the at **GTC sample**.



# CIV $\lambda 1549$ outflows and the Eddington ratios

Moreover, the Pop. A sources tend to show high luminosities and Eddington ratios.



## Conclusions

- 4DE1 criteria are good in the selections of highly accretor quasars (type 1 AGNs)
- Blueshift components contribute more than 40% of the flux in 65% of our sources
- BLR radii computed with the photoionization method are somewhat smaller than the radii derived from reverberation mapping scaling laws. And then, the black hole mass is larger.
- We confirm that these sources show a tendency to have high Eddington Ratios